

Signaling and Expression for Mitochondrial Membrane Proteins During Left Ventricular Remodeling and Contractile Failure After Myocardial Infarction

Xue-Han Ning, MD,* Jianyi Zhang, MD, PhD,† Jingbo Liu, MD, PhD,† Yun Ye, MD,† Shi-Han Chen, PhD,* Arthur H. L. From, MD,† Robert J. Bache, MD, FACC,† Michael A. Portman, MD, FACC*

Seattle, Washington and Minneapolis, Minnesota

OBJECTIVES	This study was conducted to test hypotheses stating that: 1) altered signaling for mitochondrial membrane proteins occurs during postinfarction remodeling, and 2) successful myocardial adaptation relates to promotion of specific mitochondrial membrane components.
BACKGROUND	Abnormalities in high-energy phosphate content and limitations in adenosine 5'-triphosphate (ATP) synthesis rate occur during the transition to contractile failure from compensatory remodeling after left ventricular infarction. The adenine nucleotide translocator (ANT) and F1-ATPase respectively regulate mitochondrial adenosine 5'-diphosphate (ADP)/ATP exchange and ADP-phosphorylation, which are key components of high-energy phosphate metabolism.
METHODS	Steady-state mRNA and protein expression for ANT isoform1 and the beta subunit of the F1-ATPase (betaF1) were analyzed in myocardium remote from the infarction zone eight weeks after left circumflex coronary artery ligation in pigs, demonstrating either successful left ventricular remodeling (LVR, n = 8) or congestive heart failure (CHF, n = 4) as determined by clinical and contractile performance parameters.
RESULTS	Substantial reductions in steady-state mRNA expression for ANT1 and betaF1 relative to normal (n = 8) occur in CHF, p < 0.01, but not in LVR. Relative expression for both proteins coordinated with their respective steady-state mRNA levels; CHF at 40% normal, p < 0.05 for ANT and 70% normal for betaF1, p < 0.05.
CONCLUSIONS	Maintained signaling for major mitochondrial membrane proteins occurs in association with successful remodeling and adaptation after infarction. Reduced expression of these proteins relates to limited ATP synthesis capacity and high energy phosphate kinetic abnormalities previously demonstrated in CHF. These findings imply that mitochondrial processes participate in myocardial remodeling after infarction. (J Am Coll Cardiol 2000;36:282-7) © 2000 by the American College of Cardiology

Myocardial remodeling occurs after left ventricular (LV) infarction in areas remote from the injury site (1,2). This remodeling presumably represents an effort to compensate for changes in mechanical stress caused by localized cell death and necrosis within the infarcted myocardium. The precise mechanisms, which cause the transition to contractile failure from compensatory ventricular remodeling, have not been defined (1,2). Alterations in gene and protein expression induced by changes in cardiac mechanical stretch appear to play a major role in these processes (3,4). Changes in expression have been related to contractile proteins as well as components of the sarcoplasmic reticulum and membrane receptors (2). Although abnormalities in coupling between energy utilization and production might contribute to contractile failure, neither signaling specific

mitochondrial proteins nor expression have been examined during postinfarction myocardial remodeling.

The final component of the reaction sequence linking carbon substrate utilization to oxidative phosphorylation is the mitochondrial F1-F0-ATPase; this enzyme catalyzes phosphorylation of adenosine 5'-diphosphate (ADP) to form adenosine 5'-triphosphate (ATP) (5). Because the inner mitochondrial membrane is not permeable to adenine nucleotides, exchange of ADP for ATP produced within the intramitochondrial matrix occurs via the adenine nucleotide translocator (ANT), which spans the inner mitochondrial membrane (5). The ANT (isoform 1) and the beta subunit of the F1-ATPase represent major cardiac constitutive mitochondrial membrane proteins. The genes regulating these proteins in the heart are nuclear encoded, coordinately expressed and developmentally regulated (6). Furthermore, reductions in these transcript and protein levels relate directly to the degree of myocardial dysfunction during several pathological processes (7,8). Accordingly, we hypothesized that alterations in signaling and expression for these mitochondrial membrane proteins occur in remodeled failing hearts (congestive heart failure [CHF]), and success-

From the *Cardiology Division, Department of Pediatrics, University of Washington, Seattle, Washington; †Department of Medicine, University of Minnesota Health Sciences Center, Minneapolis, Minnesota; and the Department of Veterans Affairs Medical Center, Minneapolis, Minnesota. This work was supported by U.S. Public Health Service Grants HL 60666, HL21872, HL33600 and HL50470.

Manuscript received June 25, 1999; revised manuscript received January 17, 2000, accepted March 6, 2000.

Abbreviations and Acronyms

ADP	=	adenosine 5'-diphosphate
ANT	=	adenine nucleotide translocator
ATP	=	adenosine 5'-triphosphate
cDNA	=	complementary DNA
CHF	=	congestive heart failure
CK	=	creatine kinase
G3PDH	=	glyceraldehol-3-phosphate dehydrogenase
LCX	=	left circumflex coronary artery
LV	=	left ventricle or ventricular
LVR	=	left ventricular remodeling
SDS	=	sodium dodecyl sulfate

ful myocardial adaptation after infarction depends, in part, on promotion of these components. We examined steady-state mRNA levels for these two genes and expression for their corresponding proteins in porcine myocardium after LV infarction and remodeling induced by left circumflex artery ligation. This clinically relevant experimental model has been previously characterized with elevations in LV systolic and diastolic wall stresses and reduced systolic performance (9,10). These functional abnormalities are accompanied by reductions in steady-state high energy phosphate levels and alterations in regulation of myocardial oxidative phosphorylation (9,10).

METHODS

All experimental procedures were approved by the University of Minnesota Animal Care Committee. The investigation conformed to the "Guide for the Care and Use of Laboratory Animals" published by the US National Institutes of Health (NIH publication #85-23, revised 1985).

Infarct production by coronary ligation. This animal model of LV remodeling (LVR) has been described in detail previously (9,10). Briefly, young Yorkshire swine (45 days; ~10 kg) were anesthetized with sodium pentobarbital (30 mg/kg, IV), intubated, ventilated with a respirator and given supplemental oxygen. Arterial blood gases were maintained within the physiologic range by adjustments of the respirator settings and oxygen flow. A left thoracotomy was performed and 0.5 cm of the proximal left circumflex coronary artery (LCX) was dissected free and completely occluded with a ligature. After coronary ligation the animals were observed in the open chest state for 60 min. When ventricular fibrillation occurred, electrical defibrillation was performed immediately. This procedure was usually successful. The chest was then closed; if the heart was dilated, the pericardium was left open. The animals were given standard postoperative care, including analgesia, until they were normally active. Left circumflex coronary artery occlusion was performed in 15 pigs. Four of the 15 pigs suffered sudden death during the first week after ligation, likely secondary to ventricular arrhythmia. Studies were performed in the remaining 11 pigs eight weeks after the LCX occlusion.

Experimental preparation. Eleven pigs with LVR and eight size matched normal control animals were anesthetized with sodium alpha-chloralose (100 mg/kg followed by an infusion of 20 mg/kg/h IV), intubated, ventilated with a respirator and given supplemental oxygen. Arterial blood gases were maintained within the physiologic range by adjustments of the respirator settings and oxygen flow. A sternotomy was performed and the heart suspended in a pericardial cradle. A second heparin-filled catheter was introduced into the LV through the apical dimple and secured with a purse string suture.

Experimental protocol. Aortic and LV pressures were monitored using pressure transducers (Spectramed Inc., Oxnard, California) positioned at midchest level and recorded on an eight-channel direct writing recorder (Coulbourn Instrument Company, Lehigh Valley, Pennsylvania). Left ventricular pressure was recorded at normal and high gain for measurement of end-diastolic pressure. After completion of hemodynamic measurements, several myocardial specimens were obtained from the left anterior descending perfused region and rapidly frozen in liquid nitrogen. Tissue samples were stored at -80°C for later molecular measurements. The hearts were then excised and fixed in 10% buffered formalin. The atria, right ventricle, aorta and large epicardial vessels were dissected from the LV. The infarct scar was dissected from the LV and weighed separately from the remainder of the LV.

RNA isolation. Approximately 100 mg frozen tissue was pulverized, homogenized and total RNA extracted with an RNA Isolation Kit (Ambion Inc., Austin, Texas). The purity and concentration of the RNA samples were tested by ultraviolet absorption at A260/A280. The quality and concentration of the RNA samples were confirmed by electrophoresis on denatured 1% agarose gels (8).

Northern blot analysis. For Northern blot analysis, 15 μg of RNA was denatured and electrophoresed on 1% formaldehyde agarose gel, transferred to a nitrocellulose transfer membrane (Micron Separations Inc., Westboro, Massachusetts) and cross-linked to the membrane using an ultraviolet cross linker. The prehybridizing and hybridizing solutions contained 50% formamide, $1\times$ Denhardt's solution, $6\times$ saline-sodium phosphate-ethylenediaminetetraacetic acid and 1% sodium dodecyl sulfate (SDS). Complementary DNA (cDNA) probes were labeled with $[^{32}\text{P}]\text{dCTP}$ by random primer extension (PRIME-IT II, Stratagene, La Jolla, California) and added to the hybridizing solution at 1×10^6 cpm/ml. Hybridization was carried out at 42°C for 18 h. Blots were then washed several times with a final wash in $1\times$ standard sodium citrate and 0.1% SDS at 65°C . The relative contents of mRNAs were determined using a PhosphorImager Model 400S and ImageQuant quantitation software (Molecular Dynamics, Sunnyvale, California). The same size area of each band was taken to measure the intensity, and a similar area at the closest upstream position of each band was used as background (8). The blots were also exposed on Kodak X-omat film (Eastman Kodak Co.,

Table 1. Anatomic Data

	n	BW (kg) (g)	LVW (g)	LVW/BW (g/kg)	RVW/BW (g/kg)	ScarW (g)	ScarW/LVW
Normal	8	23.4 ± 3.0	63.2 ± 7.1	2.7 ± 0.3	0.92 ± 0.09		
LVR	7	25.6 ± 4.7	84.4 ± 9.0*	3.3 ± 0.4*	1.31 ± 0.09**	6.3 ± 1.0	0.07 ± 0.02
CHF	4	19.9 ± 3.0	82.9 ± 9.7*	4.0 ± 0.5**	1.66 ± 0.23**	10.1 ± 1.3	0.12 ± 0.02

Values are mean ± SEM.

BW = body weight; CHF = congestive heart failure; LVR = left ventricular remodeling; LVW = left ventricular weight; RVW = right ventricular weight; ScarW = scar weight.

*p < 0.05 vs. normal; **p < 0.01 vs. normal.

Rochester, New York) at -70°C. RNA loading was normalized by comparison with the glyceraldehyol-3-phosphate dehydrogenase (G3PDH) RNA. Adenine nucleotide translocator-1 mRNA levels were detected using a 1.4 kb cDNA fragment cloned from human skeletal muscle (ATCC, Rockville, Maryland). Beta-F1-ATPase mRNA levels were detected using a 1.8 kb cDNA fragment cloned from human HeLa cell line (ATCC, Rockville, Maryland) (8). To compare different mRNA levels in the same myocardial sample, aliquots of 15 µg total RNA from myocardium were analyzed by means of sequentially reprobing the membranes with G3PDH, ANT-1 and beta-F1-ATPase cDNA probes.

Western blot analysis. Frozen tissue (50 mg) was pulverized and homogenized in boiling 2% SDS extract solution containing 1 M urea and 10 mM Tris (hydroxymethyl) aminomethane (pH 7.5). The homogenates were centrifuged at 2,500 g. Supernatant protein concentration was calculated from the formula: protein (mg/ml) = gamma × A 205, where gamma is the coefficient determined by the spectrophotometer with standard solution at ultraviolet wavelength 205 nm. Aliquots of the aforementioned supernatant containing 100 µg of protein were fractionated in SDS, resolved by 12.5% polyacrylamide gels and transferred to polyvinylidene difluoride membranes (BioRad, Hercules, California). Rabbit antisera to rat heart ANT or rabbit antisera to purified rat liver mitochondrial beta-F1-ATPase were used for Western blot analyses (7). The immunoreactive protein was visualized with goat anti-rabbit horseradish peroxidase conjugate. All blots were developed with the SuperSignal Substrate System (Pierce, Rockfort, Illinois). Intensities for the ANT and beta-F1-ATPase bands were performed with laser densitometric scanning for relative quantitation among normal, LVR and CHF hearts. For the purpose of standardization, the same amount of protein was run in parallel lanes on SDS gel, and densitometric scanning

was performed to insure that there were no differences in the amount of protein loaded per lane.

Data analysis. Comparisons of LVR and CHF with normal were performed using one way analysis of variance or Dunnet's modification of the t test (11). A value of p < 0.05 was required for significance. All values are expressed as mean ± standard error.

RESULTS

Anatomic data. Within the LCX ligation group, four pigs had peripheral cyanosis or ascites and other evidence of CHF. Based on these clinical criteria, these four animals comprised the CHF group. The remaining seven swine formed the LVR group. The anatomic data are summarized in Table 1. In the seven LVR swine, the LV weight to body weight ratio was increased 22% as compared with eight size matched normal swine (p < 0.05). The four CHF swine demonstrated a greater degree of hypertrophy, with the LV weight to body weight ratio increased 48% as compared with the respective controls (p < 0.01). In the LVR group, scar accounted for 7% of the LV mass, while in the CHF group scar was 12% of the LV mass. Right ventricular weight to body weight ratios were increased in both experimental groups (p < 0.01).

Hemodynamic data. Hemodynamic data are shown in Table 2. In swine with compensated LVR, none of the systemic hemodynamic variables were significantly different from normal (Table 2). However, in swine with CHF, LV systolic pressure was significantly lower and LV end-diastolic pressure was significantly higher than normal (Table 2, p < 0.05).

Steady-state mRNA levels. A representative Northern blot, illustrated in Figure 1, demonstrates the bands for ANT1, beta-F1-ATPase and G3PDH. Figure 2 summarizes the steady state mRNA levels normalized to G3PDH

Table 2. Hemodynamic Data

	n	Heart Rate (beats/min)	Mean Aortic Pressure (mm Hg)	LV Systolic Pressure (mm Hg)	LV End-Diastolic Pressure (mm Hg)
Baseline					
Normal	8	128 ± 1.4	71 ± 8	96 ± 12	6 ± 1
LVR	7	139 ± 15	74 ± 8	98 ± 11	9 ± 1
CHF	4	141 ± 19	63 ± 9	72 ± 17**	16 ± 4*

Values are mean ± SEM.

CHF = congestive heart failure; LV = left ventricle; LVR = left ventricular remodeling.

*p < 0.05 in comparison with normals; **p < 0.01 in comparison with normals.

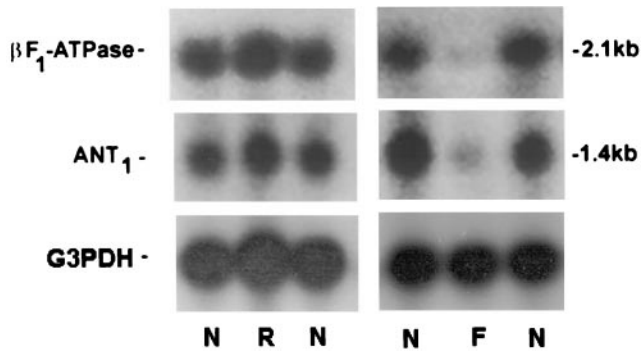


Figure 1. A representative Northern blot. Each lane represents a different heart. Lanes were loaded with 15 μg total RNA from ventricular myocardium and probed specifically for, $\beta\text{-F}_1\text{-ATPase}$, ANT-1 and G3PDH. Samples were taken from the normal heart (N), the heart with postinfarction left ventricular remodeling (R) without failure and the heart with postinfarction left ventricular failure (F) (see text). ANT = adenine nucleotide translocator.

band intensity. Normalized beta-F1-ATPase and ANT_1 mRNA levels were significantly lower in the CHF group. These levels trended higher in LVR hearts than in control, but statistical significance was not achieved.

Protein levels. Protein levels for ANT-1 and betaF1-ATPase were assessed semiquantitatively by Western blotting. A representative Western blot is shown in Figure 3. Relative normalized densitometric intensities are summarized in Figure 4. Both ANT and beta-F1-ATPase protein levels were decreased in the CHF group versus normal (0.39 ± 0.07 and 0.75 ± 0.09 , respectively, vs. 1.00 ± 0.11 and 1.00 ± 0.05 ; each $p < 0.05$), while values in the remodeled hearts were not different from control (1.01 ± 0.10 and 1.06 ± 0.05 , respectively). The relative differences in protein levels corresponded to mRNA levels, indicating coordination between message level and protein expression.

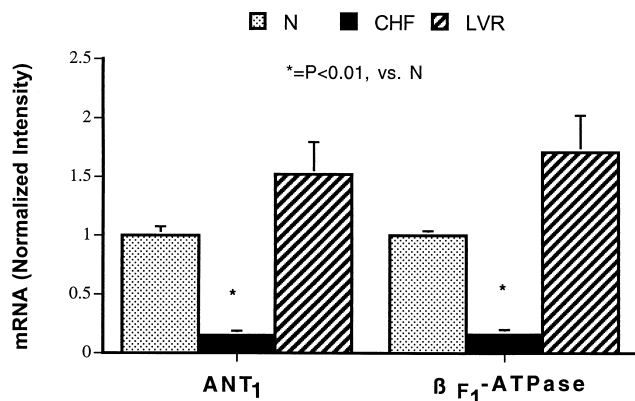


Figure 2. Steady state mRNA levels. All transcript levels are relative to the G3PDH band intensity and normalized to the lane of the normal heart. Groups are N, normal; LVR, left ventricular remodeling and CHF, congestive heart failure. The data indicate that a significant decrease in these transcript levels occurs in CHF. ANT = adenine nucleotide translocator.

Mitochondrial Proteins in Remodeled Left Ventricle

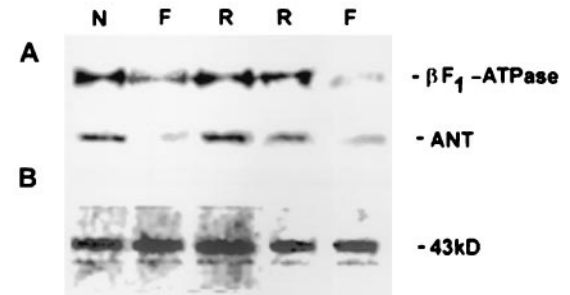


Figure 3. Representative Western blots show relative amounts of mitochondrial ANT and $\beta\text{-F}_1\text{-ATPase}$ in left ventricular myocardium in three different states (N, F, and R). Each lane represents a different heart. Substantial decreases in both mitochondrial proteins occur with heart failure (F). 43 kD protein band serves as a marker. The same amount of total protein (100 μg) was run in parallel lanes on a SDS gel for standardization purpose. ANT = adenine nucleotide translocator; F = heart with postinfarction left ventricular failure; N = normal heart; R = heart with postinfarction left ventricular remodeling.

DISCUSSION

This study provides data that support the hypothesis that an alteration in gene programming for inner mitochondrial membrane proteins occurs with decompensation after myocardial infarction. The present experimental model employing coronary artery occlusion is characterized by prominent remodeling of noninfarcted myocardium. Left ventricular chamber enlargement occurs with associated elongation and hypertrophy of isolated myocytes on histologic examination (9,10). Adjustments in cytosolic high energy phosphate concentrations and in regulation of myocardial oxidative phosphorylation accompany these morphologic and histologic changes in porcine heart. Concomitant contractile function and bioenergetic abnormalities are most prominent in failing remodeled hearts (9,10). Remodeled hearts, exhibiting LV compensation, respond normally to the stresses of rapid pacing or catecholamine infusion (10). In contrast, decompensated or failing remodeled hearts do not tolerate rapid pacing and exhibit blunting in catecholamine induced inotropy (10). Reduced catecholamine sensitivity and

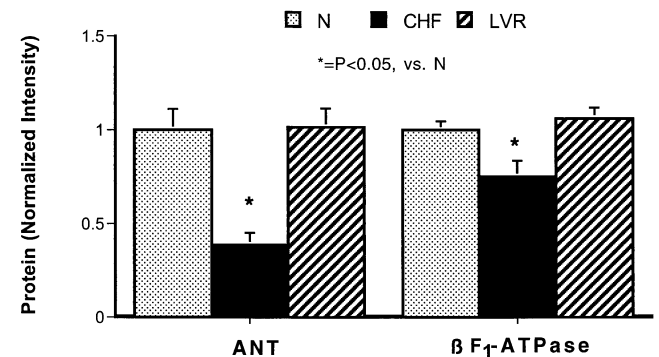


Figure 4. Densitometric intensities for protein bands from Western blots are normalized to the lane of the normal heart. The data indicate that a significant decrease in protein expression for ANT and $\beta\text{-F}_1\text{-ATPase}$ occurs in CHF. ANT = adenine nucleotide translocator; CHF = congestive heart failure; LVR = left ventricular remodeling; N = normal heart.

myosin-ATPase activity might contribute to these abnormal responses. Limitation in inherent mitochondrial oxidative capacity offers an alternative or ancillary mechanism, which can explain the failing heart's inability to increase the oxidative phosphorylation rate.

Mitochondrial proteins and contractile failure. Examination of expression for the ANT and a major subunit of the mitochondrial (F1-F0) ATPase represent a novel approach to evaluating the bioenergetic response during myocardial remodeling and failure. However, establishing direct causative linkage between specific mitochondrial proteins and contractile failure represents a challenge, as several components comprise the oxidative phosphorylation process. Several investigators have previously tested alternative candidate sites for disruption of mitochondrial respiration in remodeled myocardium remote from the infarction site (12-14). Although the creatine kinase (CK) system has received considerable attention, the implications of CK abnormalities in remodeled myocardium have not been totally defined. Neubauer and colleagues (12) found reductions in CK flux in association with reestablishment of fetal isozyme profiles in residual intact myocardium from chronically infarcted rats (12). Similar CK isoform distribution and flux abnormalities occur in the current porcine model (10,13). Despite these reductions, cytosolic CK fluxes in both rat and porcine remodeled myocardium remain substantially higher than the concurrent ATP synthesis rate. Thus, these CK enzyme system disturbances probably do not cause limitations in ATP synthesis capacity although they may alter the apparent kinetic characteristics of oxidative phosphorylation and shift sites of respiratory control.

ANT deficiency and high energy phosphate abnormalities. The ANT provides another potential site for disruption of myocardial respiration in remodeled or failing myocardium. Deficits in myocardial ANT transcript levels, protein content or carrier activity occur in several models of CHF and myocardial stunning (8,15,16). Kinetic studies performed in isolated mitochondria and using ³¹P magnetic resonance spectroscopy in the heart in vivo suggest that ANT deficiencies can cause alterations in respiratory control mechanisms (7,17,18). Thus, immature cardiac mitochondria, which are low in ANT relative to their adult counterparts, require correspondingly higher levels of ADP to drive respiration (7,17). Previously published studies employing the current pig model demonstrated substantially lower myocardial PCr/ATP and, thus, higher ADP concentrations in CHF than in LVR or control, despite similar rates of ATP synthesis (10). Furthermore, the oxygen consumption response to inotropic stimulation was extremely limited in CHF hearts, implying that markedly elevated ADP concentrations are required to maintain ambient levels of oxygen consumption. Thus, these data support the contention that ANT deficit is linked to the high energy phosphate abnormalities and the limited respiratory capacity noted in CHF hearts.

Beta-F1-ATPase and myocardial oxygen consumption rate. The current data also demonstrate a decrease in beta-F1-ATPase protein in remodeled myocardium showing evidence of contractile failure. Although protein expression does not necessarily correspond to enzyme activity, beta subunit content does correlate with F1-ATPase activity in isolated mitochondria (19). Studies performed in canine myocardium in vivo show a direct relationship between mitochondrial ATPase activity and myocardial oxygen consumption rate, though not with a 1:1 stoichiometry (20). Therefore, one can logically assume that decreased beta subunit protein content can limit ATP synthase capacity. Such a deficit might contribute to the apparent reduction in the dobutamine inducible rate of myocardial oxygen consumption, as well to the alterations in high energy phosphate levels previously observed in failing pig myocardium (10).

The relation between mitochondrial protein expression and mRNA levels. Coordination between protein expression and steady-state mRNA levels occurs for both the ANT and beta-F1-ATPase in this model. This implies that regulation of these proteins depends, in part, on changes in transcriptional rates and/or in stability of transcriptional products. Preserved expression of these genes occurs with successful LV compensation after infarction, while downregulation occurs with contractile failure in this porcine model. The importance of mitochondrial stability and maintenance of signaling for these prominent mitochondrial membrane proteins has not been previously explored during postinfarction remodeling, though preservation of these signals occurs in association with preserved metabolic and contractile function after ischemic injury in the isolated perfused heart (8). The modes of regulation of the transcriptional or posttranscriptional events, which determine these transcript levels during myocardial remodeling, require elucidation. Depre and colleagues (4) have recently shown that myocardial transcript levels for the outer mitochondrial membrane protein, carnitine palmitoyltransferase I, respond to changes in mechanical stretch during myocardial remodeling induced by chronic loading or unloading. Downregulation of expression for this gene occurs in conjunction with reestablishment of fetal isoform patterns for myosin, specific growth factors and protooncogenes. Their data would imply that signals or processes regulating these factors also regulate nuclear encoded mitochondrial proteins such as those examined in this study. However, in those previous studies no distinction was made between successful compensation and maladaptation.

Conclusions. In summary, the current data show that altered accumulation of specific inner mitochondrial membrane proteins occurs during myocardial remodeling that progresses to contractile failure. These data suggest that the mitochondrial protein response influences the direction of adaptation during postinfarction remodeling. Lack of accumulation of these proteins is consistent with abnormalities in high energy phosphate metabolism previously observed in

this model. However, proof that reductions in these proteins contribute to the limitations in oxidative phosphorylation and contractile failure will require further rigorous analyses of the bioenergetic state at maximal performance in failing remodeled hearts. Remodeling may also involve changes in regulation of other mitochondrial membrane components, which are either nuclear or mitochondrial encoded. This study was not performed to exclude these other proteins, but rather to focus attention on the importance of mitochondria during remodeling. These particular proteins were chosen for study because they have been closely linked to regulation of myocardial oxidative phosphorylation. Furthermore, previous studies have not differentiated responses between clinically compensated and failing remodeled myocardium.

Reprint requests and correspondence: Michael A. Portman, Cardiology/CH11, Children's Hospital and Regional Medical Center, 4800 Sand Point Way Northeast, Seattle, Washington 98105. E-mail: mportm@chmc.org.

REFERENCES

1. Gaudron P, Eilles C, Kugler I, Ertl G. Progressive left ventricular dysfunction and remodeling after myocardial infarction. Potential mechanisms and early predictors (see comments). *Circulation* 1993; 87:755-63.
2. Swynghedauw B. Molecular mechanisms of myocardial remodeling. *Physiol Rev* 1999;79:215-62.
3. Sadoshima J, Jahn L, Takahashi T, Kulik TJ, Izumo S. Molecular characterization of the stretch-induced adaptation of cultured cardiac cells. An in vitro model of load-induced cardiac hypertrophy. *J Biol Chem* 1992;267:10551-60.
4. Depre C, Shipley GL, Chen W, et al. Unloaded heart in vivo replicates fetal gene expression of cardiac hypertrophy. *Nature Med* 1998;4: 1269-75.
5. Nichols D, Ferguson S. *Bioenergetics 2*. San Diego: Academic Press Limited, 1992.
6. Portman MA, Han S-H, Xiao Y, Ning X-H. Maturation changes in gene expression for adenine nucleotide translocator isoforms and beta-F1ATPase in rabbit heart. *Mol Gen Metab* 1999;66:75-9.
7. Portman MA, Xiao Y, Song Y, Ning X-H. Expression of adenine nucleotide translocator parallels maturation of respiratory control in vivo. *Am J Physiol* 1997;273:H1977-83.
8. Ning X-H, Xu C-S, Song Y, et al. Hypothermia preserves function and signaling for mitochondrial biogenesis during subsequent ischemia. *Am J Physiol* 1998;274:H786-93.
9. Zhang J, Wilke N, Wang Y, et al. Functional and bioenergetic consequences of postinfarction left ventricular remodeling in a new porcine model. MRI and 31 P-MRS study. *Circulation* 1996;94: 1089-100.
10. Murakami Y, Zhang J, Eijgelshoven MH, et al. Myocardial creatine kinase kinetics in hearts with postinfarction left ventricular remodeling. *Am J Physiol* 1999;276:H892-900.
11. Dunnett CW. New tables for multiple comparisons with a control. *Biometrics* 1964;20:482-91.
12. Neubauer S, Horn M, Naumann A, et al. Impairment of energy metabolism in intact residual myocardium of rat hearts with chronic myocardial infarction. *J Clin Invest* 1995;95:1092-100.
13. Hoang CD, Zhang J, Payne RM, Apple FS. Postinfarction left ventricular remodeling induces changes in creatine kinase mRNA and protein subunit levels in porcine myocardium. *Am J Pathol* 1997;151: 257-64.
14. Nascimben L, Ingwall JS, Pauletto P, et al. Creatine kinase system in failing and nonfailing human myocardium. *Circulation* 1996;94:1894-901.
15. Dorner A, Schulze K, Rauch U, Schultheiss HP. Adenine nucleotide translocator in dilated cardiomyopathy: pathophysiological alterations in expression and function. *Mol Cell Biochem* 1997;174:261-9.
16. Graham BH, Waymire KG, Cottrel B, Trounce IA, MacGregor GR, Wallace DC. A mouse model for mitochondrial myopathy and cardiomyopathy resulting from a deficiency in the heart/muscle isoform of the adenine nucleotide translocator. *Nature Genet* 1997;16: 226-34.
17. Schonfeld P, Fritz S, Halangk W, Bohensack R. Increase in the adenine nucleotide translocase protein contributes to perinatal maturation of respiration in rat liver mitochondria. *Biochim Biophys Acta* 1993;1144:353-8.
18. Schonfeld P. Expression of the ADP/ATP carrier and expansion of the mitochondria (ATP + ADP) pool contribute to postnatal maturation of the rat heart. *Eur J Biochem* 1996;241:895-900.
19. Izquierdo JM, Luis AM, Cuezva JM. Postnatal mitochondrial differentiation in rat liver. Regulation by thyroid hormones of the beta-subunit of the mitochondrial F1-ATPase complex. *J Biol Chem* 1990;265:9,090-7.
20. Scholz TD, Balban RS. Mitochondrial F1-ATPase activity of canine myocardium: effects of hypoxia and stimulation. *Am J Physiol* 1994; 266:H2396-403.